

3.3.0 Task 4. Catalyst Testing

3.3.1 Deactivation of Iron-based Catalysts for Slurry-Phase Fischer-Tropsch Synthesis

ABSTRACT

Deactivation rates and aged catalyst properties have been investigated as a function of time on stream for iron-based Fischer-Tropsch catalysts in the presence/absence of potassium and/or silicon. There is a synergism in activity maintenance with the addition of both potassium and silicon to an iron catalyst. The addition of silicon appears to stabilize the surface area of the catalyst. Catalysts containing only iron or added silicon with or without potassium consist mainly of iron oxide at the end of the run. However, iron carbides are the dominant phase of the iron catalyst with added potassium alone. Catalyst surface areas increase slightly during synthesis. The bulk phase of the catalyst does not correlate to the catalyst activity. The partial pressure of water in the reactor is lower for potassium-containing catalysts and is not a reliable predictor of catalyst deactivation rate.

INTRODUCTION

The Fischer-Tropsch Synthesis (FTS) converts synthesis gas (a mixture of CO and H₂) to hydrocarbons. Iron-based catalysts lose activity with time on stream (TOS). The rate of deactivation is dependent on the presence/absence of promoters such as potassium and/or binders such as silica [1,2]. Several possible causes of catalyst deactivation have been postulated [3]: (i) Sintering, (ii) Carbon deposition, and, (iii) Phase transformations. With respect to phase transformations, there is considerable disagreement whether the active phase for the FTS is iron oxide or carbide [4,5]. In

addition, certain reactor conditions, such as a high partial pressure of water, are known to cause a decline in activity [6].

There were two major objectives of this study. Firstly, the effects of the addition of potassium and/or silicon on catalyst deactivation rates and changes in catalyst properties with TOS were investigated. Secondly, the possible causes of catalyst deactivation were examined by following aged catalyst properties and reactor conditions as a function of TOS for each catalyst. The FTS was carried out in a continuous-flow stirred slurry reactor to ensure uniformity in catalyst aging and reactor conditions throughout the reactor. The aged catalyst properties examined as a function of TOS were total surface areas, carbon deposits and phase transformations.

EXPERIMENTAL

Four precipitated iron-based catalysts were used. The first catalyst consisted of only iron. The other catalysts contained either added potassium, added silicon or both. The catalysts were designated in terms of the atomic ratios as: 100Fe, 100Fe/3.6Si, 100Fe/0.71K and 100Fe/3.6Si/0.71K. The catalysts were prepared by continuous precipitation from iron (III) nitrate and concentrated ammonium hydroxide. For silica-containing catalysts, a colloidal suspension of tetraethyl ortho silicate was mixed with the iron nitrate solution prior to precipitation. Potassium was added to the catalysts in the form of potassium tertiary butoxide during the loading of the FTS reactor.

The FTS was carried out in a 1 liter continuous flow stirred tank slurry reactor. The vapor phase products exiting the reactor passed through two traps in series. The first trap was maintained at 100°C while the second was maintained at 0°C. The second trap served to condense almost all of the water present in the product stream. Further details of the reaction system and product analysis (both on- and off-line) have been

reported previously [7]. A known amount (~ 70 g) of the catalyst was charged to the reactor along with 300 g of a hydrocarbon oil supplied by Ethyl Corp. (carbon number range of about C₂₅ - C₃₀). The catalyst was pretreated with a continuous flow of CO at 2.0 NL/hr-gFe at 270°C, 175 psig for 24 hours. Subsequently, the FTS was carried out at 270°C, 175 psig with a synthesis gas having an H₂/CO ratio of 0.7 at a flowrate of 3.4 NL/hr-gFe. Both during pretreatment and synthesis, small amounts of catalysts (0.1 to 0.2 g per sample) were removed from the reactor at various TOS. The aged catalyst samples were Soxhlet-extracted with xylene prior to analysis. These aged catalyst samples were examined to determine BET surface areas, elemental carbon and hydrogen contents and bulk catalytic phases.

Elemental carbon and hydrogen contents were determined using a Leco CHN analyzer wherein the catalyst sample was placed in a furnace at 1350°C under flowing oxygen. All of the carbon and hydrogen in the sample was converted to CO₂ and water respectively which were then measured. Bulk catalyst phases were determined by two methods: X-ray diffraction (XRD) and Mossbauer spectroscopy (MS). X-ray diffraction patterns were obtained using a Phillips APD X-ray diffraction spectrometer equipped with a Cu anode and a Ni filter operated at 40 kV and 20 mA (CuK α =1.5418 Å). Mossbauer spectra of the catalyst samples were obtained with a constant acceleration spectrometer using a radioactive source consisting of 50 to 100 mCi of ⁵⁷Co in a Pd matrix.

RESULTS AND DISCUSSION

The conversion of synthesis gas is a measure of the FTS activity of a catalyst. The catalysts studied show varying rates of decline in synthesis gas conversion with TOS (Figure 1). Note that the conversions for different catalysts are compared at the

same synthesis gas space velocity which is defined as normal liters of synthesis gas per gram of iron in the reactor. The addition of silica alone (100Fe/3.6Si) slows the decline in FTS activity as compared to a catalyst containing only iron (100Fe). In contrast, the addition of potassium alone increases the deactivation rate as compared to a catalyst containing only iron (100Fe). The catalyst containing both silica and potassium (100Fe/3.6Si/0.71K) exhibits the lowest deactivation rate. Hence, there is a synergism in the maintenance of FTS activity with the addition of both silica and potassium.

The surface areas of the catalysts are substantially decreased during pretreatment (Figure 2). During synthesis, however, the surface area of the catalysts increases slightly. It is postulated that this slight increase may be due to the deposition of porous carbon on the catalyst surface. Catalysts containing silica exhibit higher surface areas on preparation, and during pretreatment and synthesis. Hence, silica appears to stabilize the surface area of the catalysts. Since the total surface area increases during synthesis, the presence/absence of sintering during FTS cannot be deduced from BET surface area measurements.

The catalyst sample is exposed to air for a short time during XRD and MS. However, using similar procedures Mossbauer spectra have been previously obtained showing 97% of the iron in a catalyst as iron carbide and substantial (36%) amounts of metallic iron in another catalyst [8]. Hence, re-oxidation of catalyst phases during XRD and MS is negligible. The results from XRD indicate the following events occurring during pretreatment and synthesis: The catalyst as charged into the reactor is in the form of an oxide and/or an oxyhydroxide. During pretreatment in CO, the catalyst is rapidly converted to Fe_3O_4 which is subsequently partially converted in a slow step to a

mixture of carbides (Fe_5C_2 and $\text{Fe}_{2.2}\text{C}$) as shown in Figure 3. During synthesis, the relative amounts of carbide and oxide change dependent on the catalyst composition. For the catalyst containing only potassium, the catalyst at the end of the run consists of mainly carbides (Figure 3) while for the other catalysts the oxide is the dominant phase at the end of the run (example of 100Fe given in Figure 3). These qualitative observations are consistent with quantitative results obtained by MS. Since the catalyst containing potassium alone has the highest deactivation rate, it is tempting to conclude that the iron oxide is the active phase, or at least more active than the carbide, for the FTS. However this is not true as the bulk composition of the catalyst, as shown below, does not correlate to the catalyst activity. Figure 4 shows quantitative results of the bulk composition of the catalyst obtained by MS as a function of TOS for the catalyst with the lowest deactivation rate (100Fe/3.6Si/0.71K). The results are similar to those for the catalyst containing only iron but are different from those obtained for the catalyst containing iron and potassium but no silicon. The bulk composition of the catalyst changes greatly with TOS. At small TOS, iron carbide is the dominant phase while at long TOS the catalyst consists predominantly (80%) of iron oxide. Note, however, that synthesis gas conversion for this catalyst varied only slightly (between 80 and 90%) with TOS. Hence, the particular active phase of the catalyst (oxide or carbide) cannot be deduced from bulk catalyst compositions.

The carbon measured as a result of high temperature oxidation can be due to either CH_x species on the catalyst surface, or the oxidation of iron carbides, or the oxidation of carbon deposits. The contribution of CH_x species can be estimated by elemental analysis of hydrogen and assuming the value of x to be 2. The remaining carbon measured on the catalysts (Figure 5) ranged from 10 to 30 wt.%. Note that if all

the iron in the catalyst were converted to carbide the carbon amount would be 8 to 9 wt.% assuming the iron carbides are Fe_5C_2 and $\text{Fe}_{2.2}\text{C}$ as shown by XRD and MS. Hence, substantial amounts of carbon deposits were present on the catalyst surface. The addition of potassium to the catalyst containing only iron (100Fe/0.71K) increased the amount of carbon measured as well as its rate of increase. However, this may have been due to the high amount of carbide formed on this catalyst during synthesis as shown by XRD and MS. The catalyst with the lowest deactivation rate (100Fe/3.6Si/0.71K) contained substantial amounts of carbon at the end of the run even though its activity was quite stable. Recall that this catalyst consisted mainly of iron oxide so that the carbon measured consisted mainly of carbon deposits. Hence, the amount of carbon deposits on the catalysts does not correlate with the rate of deactivation.

As stated previously, almost all of the water present in the product stream is condensed in a trap downstream of the reactor maintained at 0°C . It is further assumed that the uncondensed gases leaving the trap are saturated with water. The partial pressure of water is then calculated by measuring the total flow rate of the uncondensed gases and the composition of the other products and unconverted reactants. This procedure yields oxygen component balances of greater than 96%. The value of the partial pressure of water in the reactor depends on the presence/absence of potassium promoter (Figure 6). The partial pressure of water is low for catalysts containing potassium and decreases slightly with TOS. In contrast, the partial pressure of water is higher for catalysts without potassium and increases with TOS. Low water partial pressures for potassium-containing catalysts may be due to the higher rates of the water gas shift (WGS) reaction observed over these catalysts. A high partial

pressure of water is known to deactivate the catalyst [6]. However, the results shown in Figure 6 indicate that the value of the partial pressure of water does not correlate to the rate of catalyst deactivation. For instance, both the catalyst with the highest and lowest deactivation rates (100Fe/0.71K and 100Fe/3.6Si/0.71K respectively) exhibit similar partial pressures of water.

It has been postulated that changes in the amount of iron oxide on the catalyst surface (as opposed to the bulk followed by XRD and MS) can be followed by a comparison of the ratios of the rates of the FTS to that of the WGS with TOS [9]. It is postulated [9] that iron oxide is more active than iron carbides for the WGS than for the FTS and hence, a decrease in the ratio of the rate of the FTS to the rate of the WGS indicates an increase in the amount of iron oxide on the catalyst surface. However, none of the catalysts examined in this study show a decline in the reaction rate ratio with TOS (Figure 7). For catalysts containing potassium, the reaction rate ratio changes negligibly with TOS, while the reaction rate ratio actually increases with TOS for the catalysts without potassium. Further, the increase in the reaction rate ratio with TOS for catalysts without potassium may not be due to changes in surface phases. We have earlier shown [10] during kinetic studies that the ratio of the reaction rate of the FTS to that of the WGS increases with residence time (not TOS) or synthesis gas conversion for iron-based catalysts. Hence, the increase in the reaction rate ratio observed for two of the catalysts studied may be a consequence of decreasing synthesis gas conversion (due to deactivation) rather than a change in surface catalyst phases.

CONCLUSION

Increasing and decreasing deactivation rates of iron FTS catalysts are observed upon the addition of potassium and/or silicon respectively. There is a synergism in the

maintenance of activity with the addition of both potassium and silicon leading to a low deactivation rate.

Changes in catalyst properties and reactor conditions with TOS depend upon the presence/absence of potassium and silicon. The addition of silicon appears to stabilize the surface area of the catalyst both on preparation and during pretreatment and synthesis. At the end of pretreatment, all of the catalysts studied consist of a mixture of iron oxide (Fe_3O_4) and iron carbides (Fe_5C_2 and $\text{Fe}_{2.2}\text{C}$). During synthesis, the catalyst containing potassium alone is converted predominantly to iron carbides at the end of the run. The other catalysts, however, decline in the amount of iron carbide and increase in the amount of iron oxide during synthesis. The addition of potassium alone to an iron catalyst substantially increases the amount of carbon (from carbon deposits and carbides) measured by high temperature oxidation of aged catalyst samples. The partial pressure of water in the reactor is low and decreases with TOS for potassium-containing catalysts while it is higher and increases with TOS for the catalysts without potassium.

Possible causes of catalyst deactivation have been investigated in this study. The surface areas of aged catalyst samples increase with TOS during synthesis possibly due to porous carbon deposits. Hence, information from total surface area on sintering as a possible mechanism of deactivation is inconclusive. Measurement of the amount of carbon deposits on the catalysts by high temperature oxidation is complicated due to the contribution from iron carbides. The bulk composition of the catalyst having the lowest deactivation rate changes greatly during synthesis whereas the synthesis gas conversion changes negligibly. This implies that the catalyst bulk composition does not correlate to the rate of activity decline. The value of the partial of

water as well as its variation with TOS are similar for the catalysts with the highest and lowest deactivation rates. Hence, water partial pressure is not a reliable predictor of the catalyst deactivation rate.

REFERENCES

1. D.B. Bukur, D. Mukesh and S.A. Patel, *Ind. Eng. Chem. Res.*, 29, 194 (1990).
2. D.B. Bukur, X. Lang, D. Mukesh, W.H. Zimmerman, M.P. Rosynek and C. Li, *Ind. Eng. Chem. Res.*, 29, 1588 (1990).
3. M.E. Dry, in J.R. Anderson and M. Boudart (Eds.), *Catalysis-Science and Technology*, Vol. 1, 159-255, Springer, Berlin (1981).
4. J.P. Reymond, P. Meriaudeau and S.J. Teichner, *J. Catal.*, 75, 39 (1982).
5. G.B. Raupp and W.N. Delgass, *J. Catal.*, 58, 361 (1979).
6. C.N. Satterfield, R.T. Hanlon, S.E. Tung, Z. Zou, G.C. Papaefthymiou, *Ind. Eng. Chem. Prod. Res. Dev.*, 25, 407 (1986).
7. L. Xu, S. Bao, R.J. O'Brien, D.J. Houpt and B.H. Davis, *Fuel Sci. Tech. Int.*, 12, 1323 (1994).
8. C.-S. Huang, B. Ganguly, G.P. Huffman, F.E. Huggins and B.H. Davis, *Fuel Sci. Tech. Int.*, 11, 1289 (1993).
9. B. Jager and R. Espinoza, *Catalysis Today*, 23, 17 (1995).
10. A.P. Raje and B.H. Davis, *Catalysis Today*, (accepted for publication).

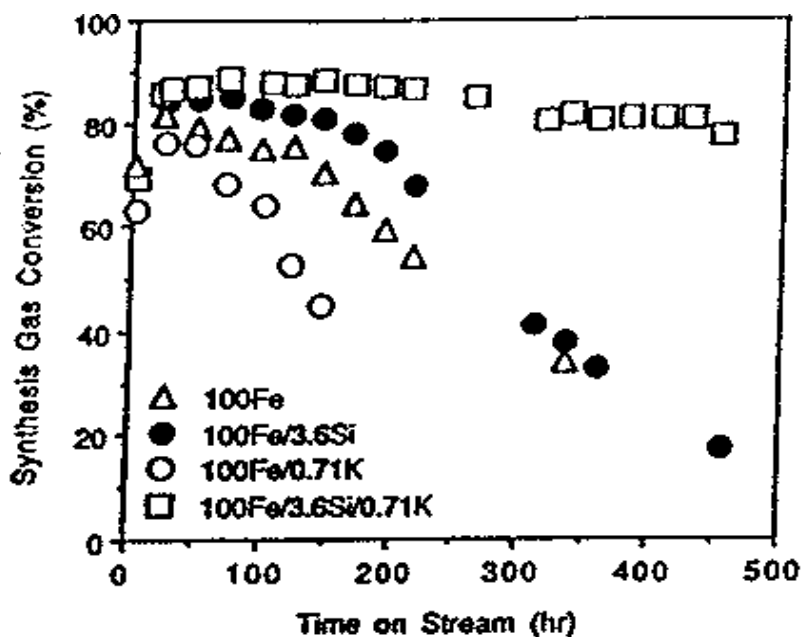


Figure 1. Synthesis gas conversion as a function of time-on-stream.

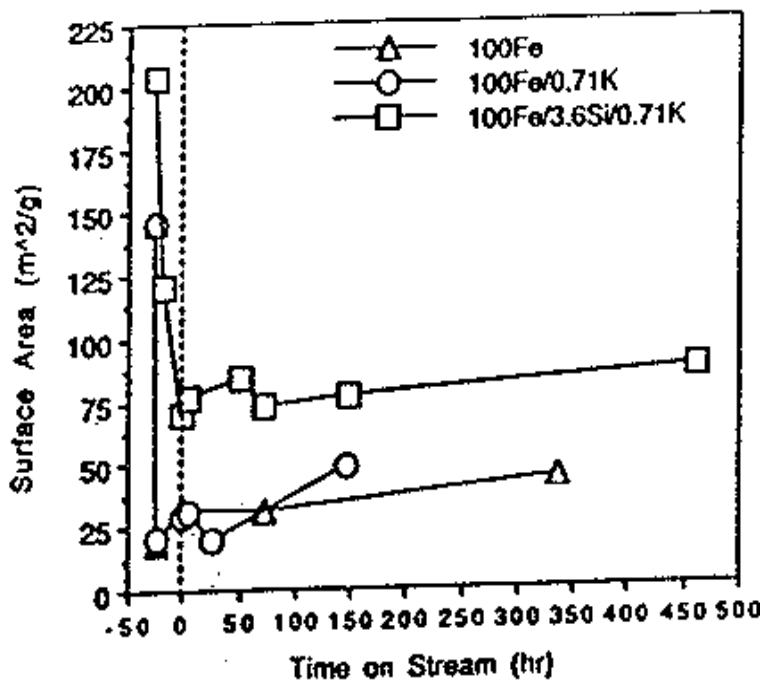


Figure 2. Catalyst surface areas as a function of time-on-stream (TOS). Negative TOS denote catalyst pretreatment; positive TOS denote Fischer-Tropsch synthesis.

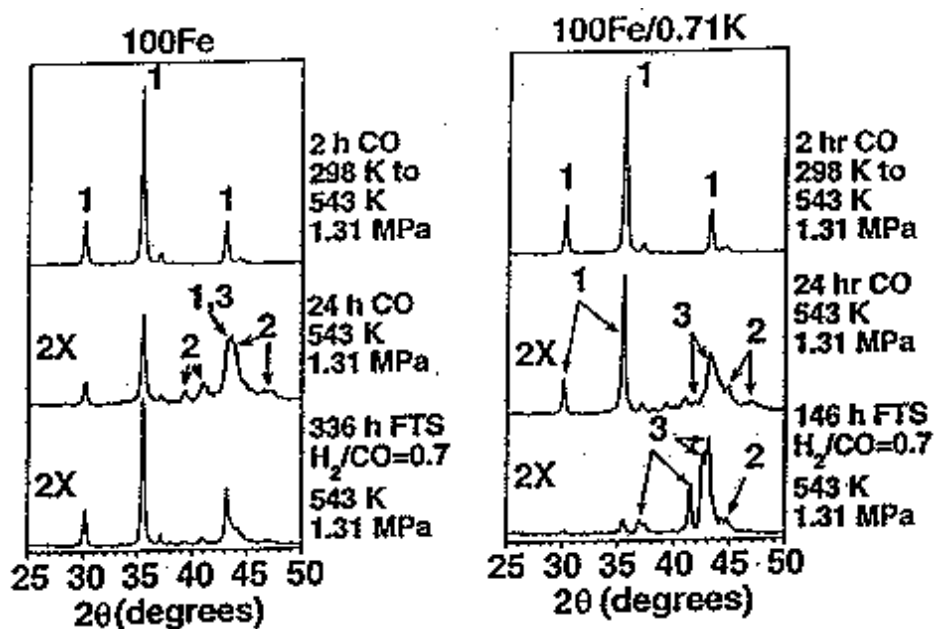


Figure 3. X-ray diffraction results for two catalysts (100Fe and 100Fe/0.71K) during pretreatment and at the end of synthesis ((1) Fe_3O_4 , (2) χ - Fe_5C_2 , (3) ϵ - $Fe_{2.2}C$).

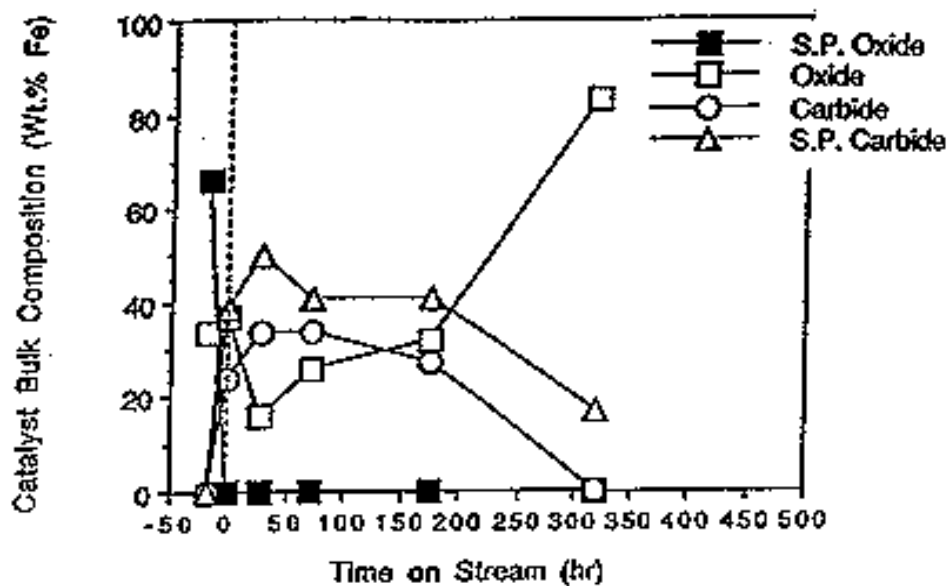


Figure 4. Bulk composition of catalyst: 100Fe/3.6Si/0.71K from Mössbauer spectroscopy as a function of time-on-stream. Negative TOS denote catalyst pretreatment; positive TOS denote Fischer-Tropsch synthesis. S.P. denotes superparamagnetic.

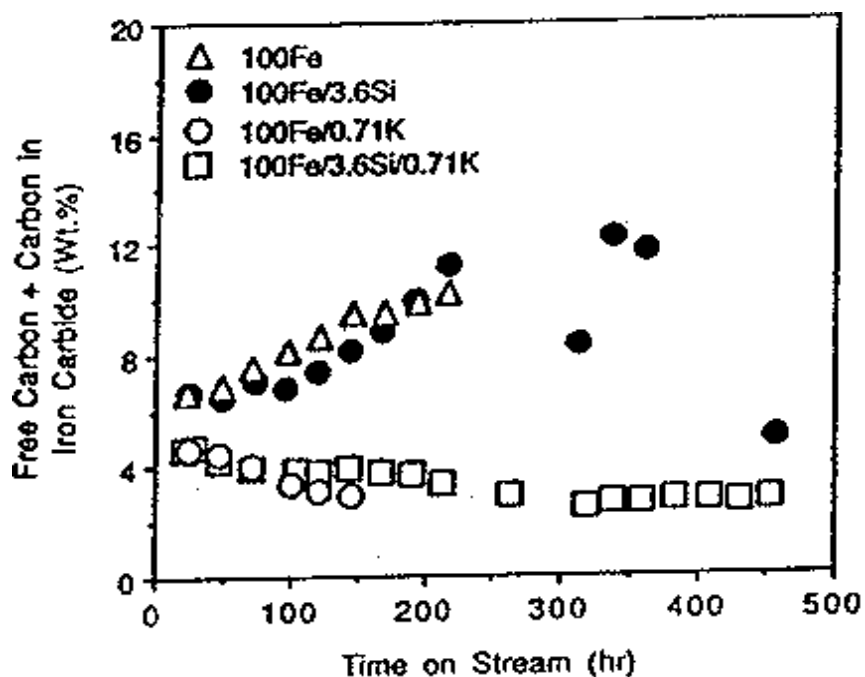


Figure 5. Amount of carbon deposits and carbon in the form of iron carbide as a function of time-on-stream (TOS). Negative TOS denotes catalyst pretreatment; positive TOS denotes Fischer-Tropsch synthesis.

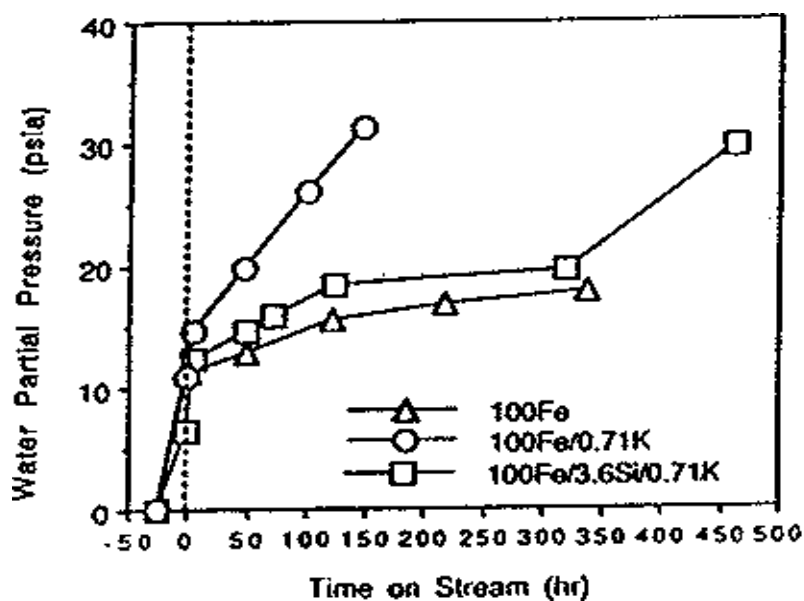


Figure 6. Partial pressure of water as a function of time-on-stream.

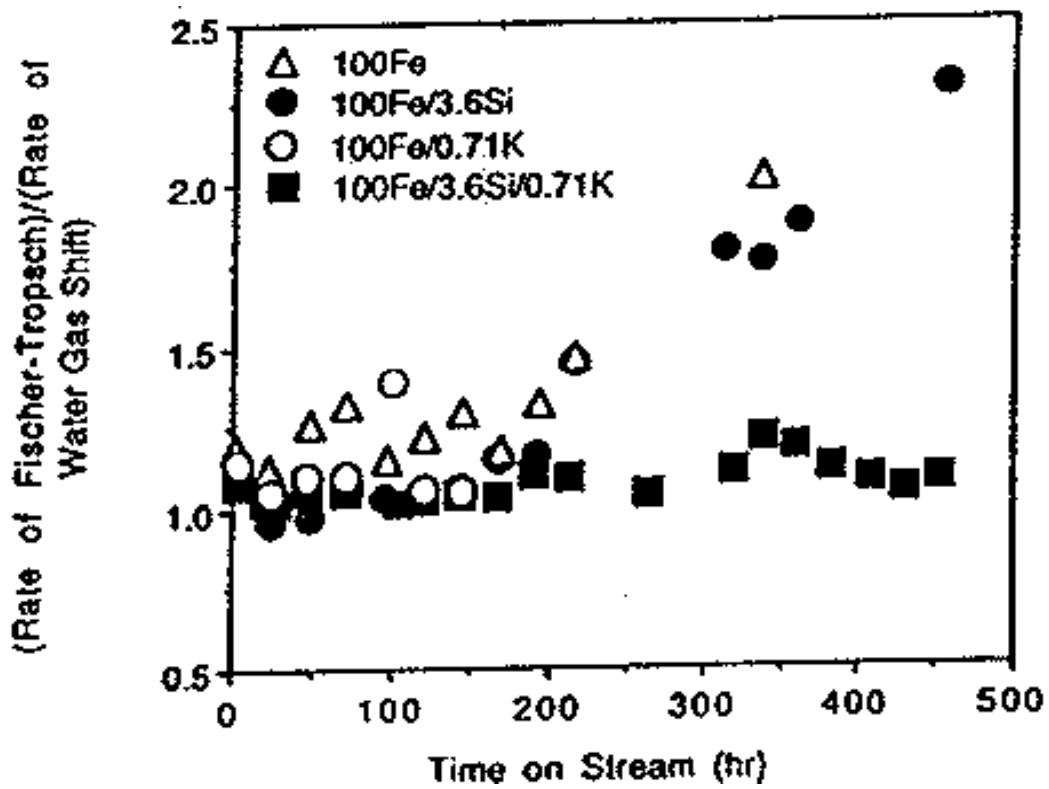


Figure 7. Ratio of the reaction rates of the Fischer-Tropsch synthesis to the water-gas shift reaction as a function of time-on-stream.

3.3.2 Fischer-Tropsch Synthesis. Conversion of Alcohols over Iron Oxide and Iron Carbide Catalysts

ABSTRACT

Both iron oxide (Fe_2O_3) and iron carbide catalysts are active for the dehydration of tertiary alcohols; the oxide catalyst is not reduced nor is the carbide oxidized by the steam generated during the dehydration reaction. Secondary alcohols are selectively converted to ketones plus hydrogen by both the iron oxide and carbide catalyst. Fe_2O_3 is reduced to Fe_3O_4 during the conversion of secondary alcohols. Both iron carbide and oxide catalysts dehydrogenate a primary alcohol (C_n) to an aldehyde; however, the aldehyde undergoes a secondary ketonization reaction to produce a symmetrical ketone with $2n-1$ carbons. These results suggest that dehydration of alcohols to produce olefins makes a minor, if any, contribution during Fischer-Tropsch synthesis with an iron catalyst at low pressure conditions.

INTRODUCTION

The conversion of syngas, a mixture of CO and H_2 , was initially believed to occur through the formation of an iron carbide which subsequently underwent hydrogenation to hydrocarbons (1). Later, a mechanism was advanced which involved the formation of an oxygen-containing surface species which underwent a series of combination-dehydration steps, ultimately leading to a primary alcohol or an alkene (2). Isotopic tracer studies by Emmett and co-workers provided data which was considered to provide strong support for the oxygen-containing intermediate (3-11). As sophisticated surface science instrumentation became available, their use showed that the metal surface was covered with carbon but that little, if any, surface oxygen could be detected. Thus, a mechanism involving the dissociation of CO to form C and O

adsorbed on the surface became widely accepted (*for example, 12-15*). In this mechanism, the adsorbed O was hydrogenated to water which rapidly desorbed while the adsorbed C was hydrogenated to form adsorbed CH, CH₂ and CH₃ groups. While any of these groups could be involved in the formation of ethylene and higher hydrocarbons, the methylene groups was considered in most mechanisms to be the surface species which underwent polymerization to produce an Anderson-Schulz-Flory distribution of hydrocarbon products.

In the case of an iron Fischer-Tropsch catalyst, the carbide phase could be formed following activation in either CO alone or with a mixture of CO/H₂ (*16,17*). In addition, any metallic iron formed by hydrogen reduction of the iron oxide catalyst precursor was quickly converted to iron carbides when the activated catalyst was exposed to the synthesis gas (*18*). However, during synthesis the iron carbide was gradually converted to a mixture containing both iron carbides and Fe₃O₄; the extent and rate of formation of the iron oxide phase depended upon the operating conditions such as CO conversion, water-gas-shift activity, promoter levels, and time-on-stream. Thus, the iron in a "working, steady-state" catalyst is present as a mixture of the oxide and carbide phases. However, while an attractive model for the working catalyst was a surface layer of iron carbide supported on a core of Fe₃O₄, data to define the structure of the working catalyst is still lacking (*19*).

Recently, isotopic tracer studies using a variety of alcohols, alkenes and carbon dioxide have produced results for iron catalysts that were consistent with a chain initiating species that contains oxygen (*20-27*). Thus, it is of interest to define the pathways for conversion of various alcohols using iron oxide and iron carbide catalysts and that is the subject of this paper.

EXPERIMENTAL

Catalyst. The iron oxide catalyst was prepared by adding concentrated ammonia to a 1M iron nitrate solution to produce a pH of about 10.5. The solid was collected and washed by repeated dispersion/filtration cycles; at the end of the washing cycles the pH was in the 7-8 range. After drying overnight at 110°C, the material had a BET surface area of 252 m²/g. The material following calcination at 300°C had an X-ray diffraction pattern consistent with α -Fe₂O₃. An iron oxide catalyst that contained 6 wt.% thoria was also prepared using a published procedure (28); this material was also α -Fe₂O₃ following calcination at 300°C.

The iron carbide catalyst was prepared by treating the α -Fe₂O₃ sample for 24 hr. in a flow of CO at 1 atm. and 300°C. Prior to use, the sample was flushed with nitrogen for 30 minutes. To obtain a sample of the carbide catalyst for X-ray analysis, the material was passivated at room temperature by passing nitrogen containing 1% oxygen over the iron carbide for about three days.

Conversions. A plug flow quartz reactor with the catalyst located in the middle was utilized. Glass beads were placed on top of the catalyst bed to serve as a preheater and a thermowell extended into the middle of the catalyst bed. During the run the alcohol was added by a syringe pump at atmospheric pressure without a diluent gas. Liquid samples were collected at appropriate intervals.

The iron oxide catalyst was activated overnight in a flow of air at 300°C prior to a run. To start a run, the air flow was terminated and the catalyst was flushed with dry nitrogen for 30 minutes. The nitrogen flow was stopped and the alcohol flow was then started. The alcohols were purchased from Aldrich and were used without purification.

The liquid samples that were collected at appropriate time intervals were analyzed by g.c. using a DB-5 column.

The iron carbide catalyst was prepared and flushed with nitrogen for about 15 minutes immediately prior to use for the alcohol conversions.

RESULTS

The conversion of 2-octanol at 275°C showed that the iron oxide catalyst was very selective for dehydrogenation but had little dehydration activity (Figure 1). Prior to the run the catalytic material was α -Fe₂O₃ (Figure 2a) but following the run the catalyst contained both α -Fe₂O₃ and Fe₃O₄ (Figure 2b). Thus, the hydrogen produced during alcohol dehydrogenation was effective in reducing the catalyst to Fe₃O₄, and the extent of reduction would presumably depend upon the length of the time that the catalyst was exposed to the flow of alcohol.

The conversion results for the thoria-containing catalyst are very similar to the run with the α -Fe₂O₃/Fe₃O₄ catalyst mixture. While the selectivity for dehydrogenation is slightly lower for the thoria containing catalyst, it has a selectivity and activity that is similar to the iron oxide catalyst (Figure 1). Following 5 hr. use as a catalyst for the conversion of 2-octanol, the X-ray diffraction pattern of this material was similar to that of the α -Fe₂O₃ catalyst that did not contain thoria (Figure 3). However, peaks at $2\theta = 31.9, 45.8$ and 66.8 , corresponding to ThO₂, were evident in the X-ray diffraction pattern for this material in addition to those for a mixture of α -Fe₂O₃/Fe₃O₄ (Figure 2c).

3-Methyl-3-pentanol, a tertiary alcohol which cannot undergo direct dehydrogenation to a ketone, was converted with the α -Fe₂O₃ catalyst. At 230°C, the catalyst was active only for dehydration to produce a mixture of cis- and trans-3-methyl-2-pentenes. Following 5 hr. use as a catalyst, the alcohol flow was terminated, the

catalyst flushed with nitrogen at reaction temperature, and then cooled to room temperature in a nitrogen flow. The X-ray diffraction pattern of the material was identical to that of the initial catalyst (Figure 3), indicating that the conversion of this tertiary alcohol did not effect any reduction of the catalyst, and this is the expected result. The conversion data for 3-methyl-3-pentanol (Figure 4) show that the tertiary alcohol is converted more rapidly than 2-octanol, a secondary alcohol.

3-Methyl-3-pentanol was also converted with an iron carbide catalyst using similar conditions as with the Fe_2O_3 catalyst except for the flow. Since the flow rate was about 1.7 times greater with the iron carbide catalyst, the iron carbide catalyst is about twice as active for 3-methyl-3-pentanol dehydration as the iron oxide catalyst is.

3-Pentanol was run at 230 and 260°C. At these two temperatures, the selectivity for dehydrogenation is almost the same although the conversion at 260°C is higher than that at 230°C. For both of these runs, the catalytic activity for 3-pentanol conversion did not decline significantly during the run (Figure 5). The X-ray diffraction pattern of the catalyst exhibited peaks corresponding to both $\alpha\text{-Fe}_2\text{O}_3$ and Fe_3O_4 following the conversion of 3-pentanol (Figure 3b) These experiments confirm that the reduction of the catalyst occurs due to exposure to the secondary alcohol.

In another run, the $\alpha\text{-Fe}_2\text{O}_3$ was reduced at 270°C for 5 hr. in a flow of hydrogen and then cooled to 230°C in hydrogen flow. A flow of 2-octanol was initiated and the flow of hydrogen was terminated. The catalyst exhibited activity for 2-octanol conversion; however, the selectivity for dehydrogenation was lower (ca. 0.83 vs. 0.96) at 230°C than at 270°C (Figure 4).

The $\alpha\text{-Fe}_2\text{O}_3$ was treated with CO at 260°C for 18 hr. to convert the iron oxide to an iron carbide. Following the treatment with CO the catalyst was flushed with nitrogen,

then a flow of 2-octanol was started and the nitrogen flow was terminated. This iron carbide catalyst had an activity and selectivity for dehydrogenation that exceeds that of the catalyst comprised of a mixture of α -Fe₂O₃ and Fe₃O₄ (Figure 6) and does not lose activity during 8 hrs. Following use as a catalyst for 8 hrs., the sample was flushed with nitrogen and cooled to room temperature. The X-ray diffraction pattern of this sample following use as a catalyst contains peaks that are consistent with both iron carbides and Fe₃O₄ (Figure 7), with the carbide being the dominant component. A chemical analysis of the sample following use as a catalyst showed that it contained 9.0 percent carbon, a value that is consistent with the sample being Fe_{2.2}C (9.67% C).

While secondary alcohols may be formed during the Fischer-Tropsch synthesis, a primary alcohol is the dominant alcohol for each carbon number. Thus, 1-octanol was converted over the iron oxide and the iron carbide catalysts. This alcohol underwent conversion by dehydrogenation to the aldehyde. The conversion increased initially and then remained essentially constant with time. The aldehyde underwent a secondary reaction that involved decarbonylation (and/or decarboxylation) to produce CO/CO₂ and the formation of a 15-carbon number symmetrical ketone. This reaction has been observed frequently during the conversion of primary alcohols with metal oxide catalysts that possess dehydrogenation properties (29). Likewise, the selectivity for 1-octanal decreased as the conversion increased. Initially 40 mole% of the products from the conversion with the catalyst was 1-octanal and the remainder was 8-pentadecanone; after the first hour 1-octanal accounted for only 26-29 mole% of the products, the remainder being 8-pentadecanone. As the activity of the iron carbide increased, the selectivity for 1-octanal decreased from 88 mole% to about 65 mole%. Thus, the iron carbide catalyst exhibited an activity for 1-octanol conversion that was about 3-4 times

that of the iron oxide catalyst and it had a selectivity for 1-octanal that was 2-2.5 times that of the iron oxide catalyst. Neither the iron oxide nor the carbide catalyzed dehydration of 1-octanol since only traces octenes were observed.

DISCUSSION

The catalytic material remains Fe_2O_3 during the conversion of 3-methyl-3-pentanol. This is not surprising since a tertiary alcohol cannot undergo dehydrogenation; rather it is dehydrated to produce an olefin and water.

The iron carbide catalyst does not undergo measurable conversion to the oxide. Likewise, the greater activity of the iron carbide, compared to Fe_2O_3 , suggests that even the surface remains the carbide during the dehydration of 3-methyl-2-pentanol and the generation of water vapor.

On the other hand, Fe_2O_3 is reduced, at least partially, to Fe_3O_4 during the conversion of secondary alcohol. However, the iron oxide is not converted to an iron carbide during the conversion of this alcohol, at least not to an extent so that the carbide phase can be detected by X-ray diffraction (XRD). The sample containing 6 wt.% ThO_2 also underwent conversion to a mixture of Fe_2O_3 and Fe_3O_4 ; in addition, a ThO_2 phase was formed so that it could be detected by XRD. This is surprising since it has been reported that when this amount of thoria is present in an iron catalyst it provided a material that had superior activity for the water-gas shift reaction than a similar material that did not contain thoria (28). It is difficult to understand why thoria should impact the activity for water gas shift if phase separation occurs in a reducing atmosphere.

If Fe_2O_3 is treated in CO to produce iron carbides, the material that remains following conversion of 2-octanol during 8 hrs is predominantly iron carbides. Thus, the

carbide is not converted to the oxide in the presence of the small amount of water produced during the dehydration of 2-octanol, primarily during the early reaction period, to an extent such that the oxide(s) can be detected by XRD.

Except during an initial break-in period, the pure iron oxide and the iron oxide sample containing 6 wt.% ThO₂ were very selective dehydrogenation catalysts for primary and secondary alcohols. Only with the tertiary alcohol, where dehydrogenation is not possible, was the iron oxide catalyst selective for dehydration.

With the secondary alcohol, the iron oxide catalyst was very selective in dehydrogenating the alcohol to the corresponding ketone. Essentially no secondary reaction products were observed.

With the primary alcohol, the iron oxide catalyst was selective for dehydrogenation to the corresponding aldehyde. However, the aldehyde underwent a secondary reaction in which it was converted to a symmetrical secondary ketone plus either CO or CO₂. This reaction is known to occur when primary alcohols are converted over a variety of metal oxide catalysts (29). In this reaction it resembles the ketonization reaction that many metal oxide catalysts effect when starting with an acid. However, the mechanism for these reactions has not been clearly elucidated to date.

The iron carbide catalyst has a selectivity that resembles that of iron oxide but it is about twice as active for the conversion of the secondary alcohols. The higher activity of the iron carbide catalyst implies that either the surface is not oxidized to the oxide during the conversion of the alcohol or the oxycarbide that is formed on the iron carbide surface is more active than the iron oxide surface. The chemical composition of the gas phase is such that the iron is expected to be present in the carbide phase (30). A similar conclusion is reached for the conversion of 1-octanol over the iron oxide and

carbide catalysts. The iron carbide is about 4 times as active for the conversion of 1-octanol as the iron oxide and has only about half the activity for the formation of a symmetrical ketone from the primary dehydrogenation product, 1-octanal.

It has been demonstrated convincingly that alcohols can serve to initiate chain growth during the Fischer-Tropsch reaction (27). Furthermore, when using a promoted iron catalyst, the alcohol incorporates into the Fischer-Tropsch products about 50-100 times greater than the alkene that would be formed from dehydration of the alcohol. The present data indicate that the primary reaction of an alcohol that is formed during the Fischer-Tropsch synthesis is to undergo dehydrogenation to the aldehyde and this is true for both Fe_3O_4 and iron carbide catalysts. The present results indicate that reincorporation of the alcohol into Fischer-Tropsch products is not through an alkene intermediate that is formed by the dehydration of the alcohol. The results are consistent with the Fischer-Tropsch mechanism requiring an initiation step that involves an oxygen-containing species, and not a surface carbon or carbene intermediate.

ACKNOWLEDGMENT

This work was supported by U.S. DOE contract number DE-AC22-94PC94055 and the Commonwealth of Kentucky.

REFERENCES

1. F. Fischer and H. Tropsch, *Zeit. fur Chem.*, **7** (1926) 97-116.
2. H. H. Storch, N. Golombic and R. B. Anderson, "The Fischer-Tropsch Synthesis," John Wiley & Sons, Inc., New York, 1951.
3. W. K. Hall, R. J. Kokes and P. H. Emmett, *J. Am. Chem. Soc.*, **79** (1957) 2983.
4. R. J. Kokes, W. K. Hall and P. H. Emmett, *J. Am. Chem. Soc.*, **79** (1957) 2089.
5. J. T. Kummer, H. Podgurski, W. B. Spencer and P. H. Emmett, *J. Am. Chem. Soc.*, **73** (1951) 564.
6. J. T. Kummer and P. H. Emmett, *J. Am. Chem. Soc.*, **75** (1953) 5177.
7. P. H. Emmett, *Oil and Gas. J.*, (Sept. 1951) 82.
8. H. H. Podgurski and P. H. Emmett, *J. Phys. Chem.*, **57** (1953) 159.
9. G. Blyholder and P. H. Emmett, *J. Phys. Chem.*, **63** (1959) 962.
10. G. Blyholder and P. H. Emmett, *J. Phys. Chem.*, **64** (1960) 470.
11. J. T. Kummer, T. W. DeWitt and P. H. Emmett, *J. Am. Chem. Soc.*, **70** (1948) 3632.
12. K. M. Sancier, W. E. Isakson and H. Wise; *ACS Symp Series*, (1979).
13. M. E. Dry, *Appl. Catal. A: General*, **138** (1996) 319-344.
14. (a) R. C. Brady, III and R. Pettit, *J. Am. Chem. Soc.*, **102**, 6181-6182 (1980); (b) R. C. Brady, III and R. Pettit, *J. Am. Chem. Soc.*, **103**, 1287-1289 (1981).
15. M. L. Turner, H. C. Long, A. Shenton, P. K. Byers and P. M. Maitlis, *Chem. Eur. J.*, **1** (1995) 549-556.
16. R. J. O'Brien, L. Xu, R. L. Spicer and B. H. Davis, *Energy & Fuels*, **10** (1996) 921-926.

17. C.-S. Huang, L. Xu and B. H. Davis, *Fuel Sci. & Tech. Intl.*, **11** (1993) 639.
18. C.-S. Huang, B. Ganguly, G. P. Huffman, F. E. Huggins and B. H. Davis, *Fuel Sci. & Tech. Intl.*, **11** (1993) 1289.
19. A. Raje, R. J. O'Brien, L. Xu and B. H. Davis, "Catalyst Deactivation 1997," (C. H. Bartholomew and G. A. Fuentes, eds.), (Studies in Surface Science Catalysis), **111**, 527 (1997).
20. H. Dabbagh, L.-M. Tau, S. Bao, J. Halasz and B. H. Davis, "Catalysis 1987" (J. Ward, Ed.) Elsevier, Amsterdam, pp. 61-72 (1988).
21. L.-M. Tau, H. Dabbagh, S. Bao, J. Halasz, B. Chawla and B. H. Davis, *Proc. 9th Int. Congr. Catal.*, **2** (1988) 861.
22. L.-M. Tau, H. A. Dabbagh and B. H. Davis, *Energy & Fuels*, **4** (1990) 94.
23. L.-M. Tau, H. A. Dabbagh and B. H. Davis, *Catal. Lett.*, **7** (1990) 141.
24. L.-M. Tau, H. Dabbagh, S. Bao and B. H. Davis, *Catal. Lett.*, **7** (1990) 127.
25. L.-M. Tau, H. A. Dabbagh and B. H. Davis, *Energy & Fuels*, **5** (1991) 174.
26. L.-M. Tau, H. A. Dabbagh, J. Halasz and B. H. Davis, *J. Mol. Cat.*, **71** (1992) 37.
27. A. Raje and B. H. Davis in "Catalysis" (J. J. Spring Ed), The Royal Soc. Chem., Cambridge, **12**, 52-131 (1996).
28. F. Domka and I. Wolska, *Surf. and Coatings Technol.*, **28**, (1986) 187.
29. V. I. Komarewsky and J. R. Coley, *Advan. Catal.*, **8** (1956) 207.
30. S.-J. Liaw and B. H. Davis, submitted.

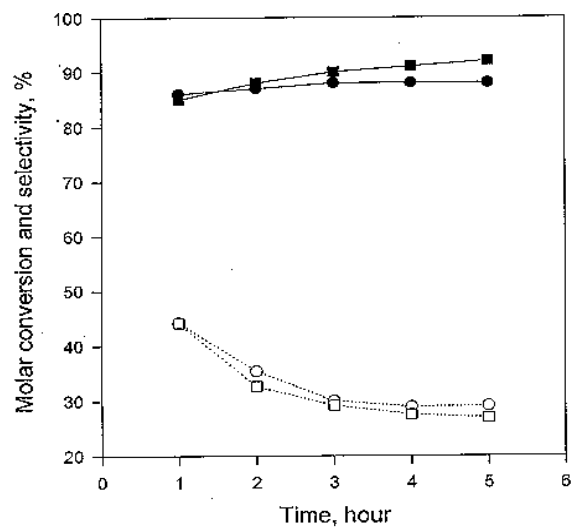


Figure 1. The conversion of 2-octanol for the Fe₂O₃ (□) and Fe₂O₃-ThO₂ (○) catalysts and the selectivity for dehydrogenation for the Fe₂O₃ (■) and Fe₂O₃-ThO₂ (●) catalysts [275°C, 1 atm, LHSV = 3.2 h⁻¹].

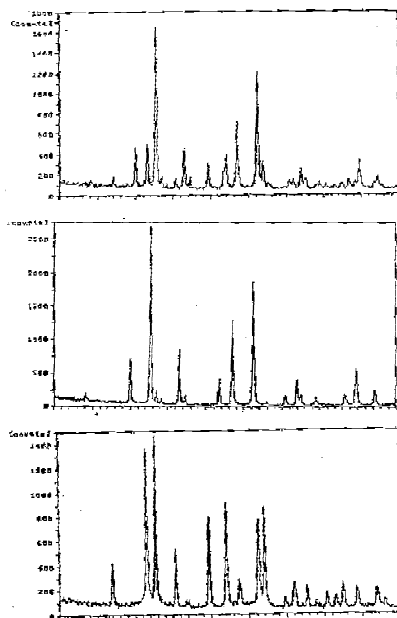


Figure 2. The X-ray diffraction patterns for: (a) the Fe₂O₃ catalyst (bottom); (b) the Fe₂O₃ catalyst after use for the conversion of 2-octanol (middle), and (c) the thoria containing catalyst after use for the conversion of 2-octanol (top).

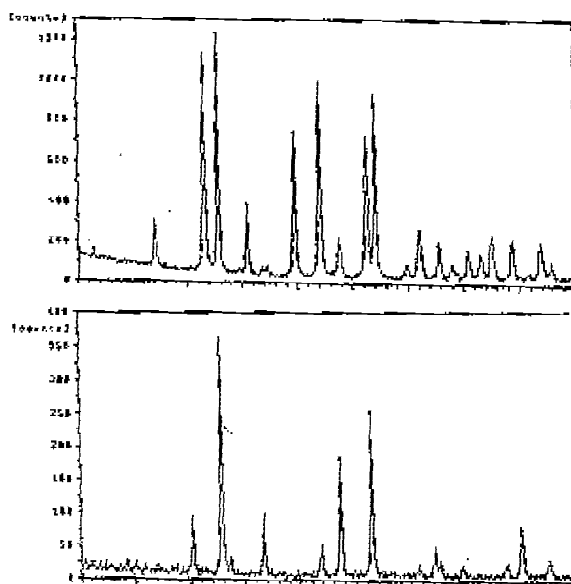


Figure 3. The X-ray diffraction pattern for the Fe_2O_3 catalyst following (a) use for the conversion of 3-methyl-3-pentanol (top) and (b) of Fe_2O_3 following use for the conversion of 3-pentanol (bottom).

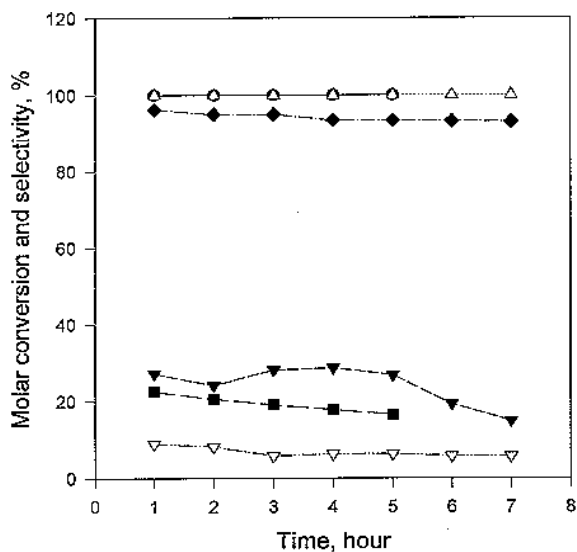


Figure 4. The conversion (∇) and dehydrogenation selectivity (\blacklozenge) for 3-pentanol ($\text{LHSV} = 1.5 \text{ h}^{-1}$) with the Fe_2O_3 catalyst; the conversion (\blacksquare) and dehydration selectivity (\bullet) for 3-methyl-3-pentanol ($\text{LHSV} = 3.2 \text{ h}^{-1}$) with the Fe_2O_3 catalyst; and the conversion (\blacktriangledown) and dehydration selectivity (\triangle) for 3-methyl-3-pentanol ($\text{LHSV} = 5.4 \text{ h}^{-1}$) the iron carbide catalyst (230°C , 1 atm).

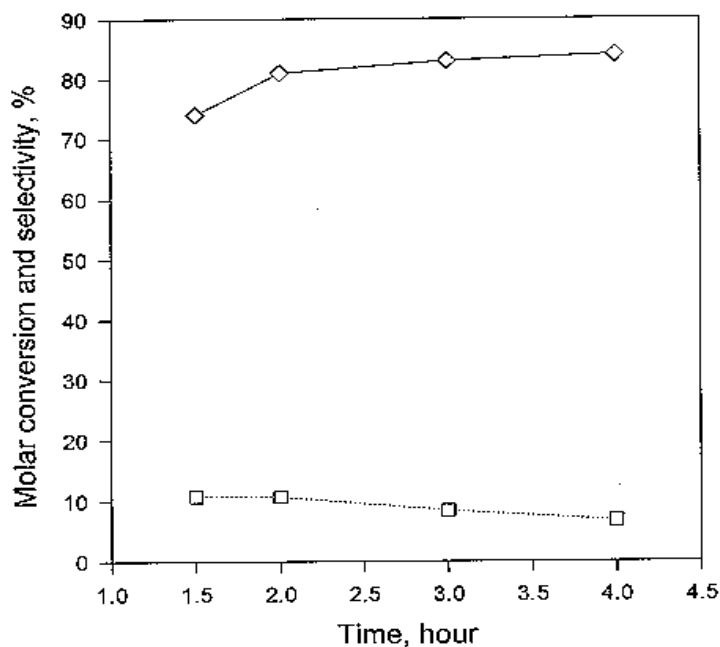


Figure 5. The conversion (□) and dehydrogenation selectivity (◇) for the Fe_2O_3 catalyst following reduction in hydrogen at 230°C , 1 atm, $\text{LHSV} = 1.5 \text{ h}^{-1}$.

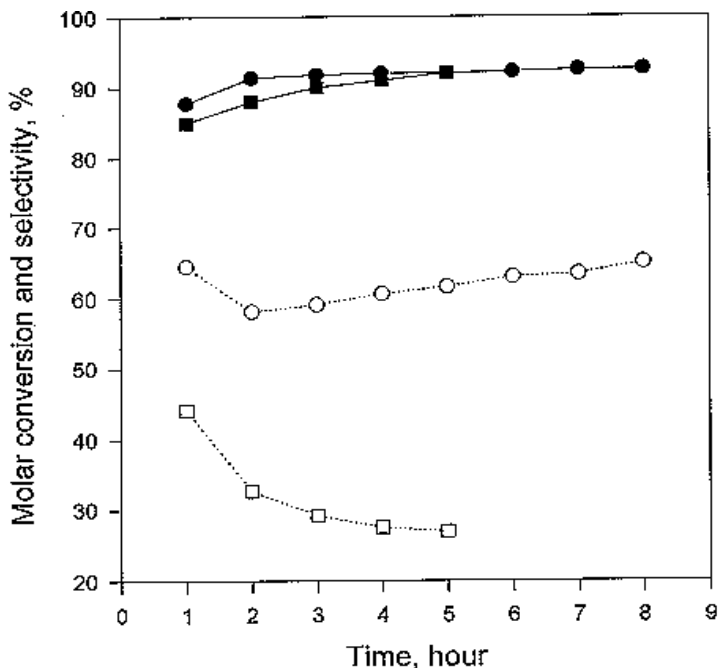


Figure 6. Conversion of 2-octanol with Fe_2O_3 (275°C , 1 atm, $\text{LHSV} = 3.2 \text{ h}^{-1}$) (□) and iron carbide (275°C , 1 atm, $\text{LHSV} = 3.2 \text{ h}^{-1}$) (○) and the dehydrogenation selectivity with Fe_2O_3 (■) and iron carbide (●).

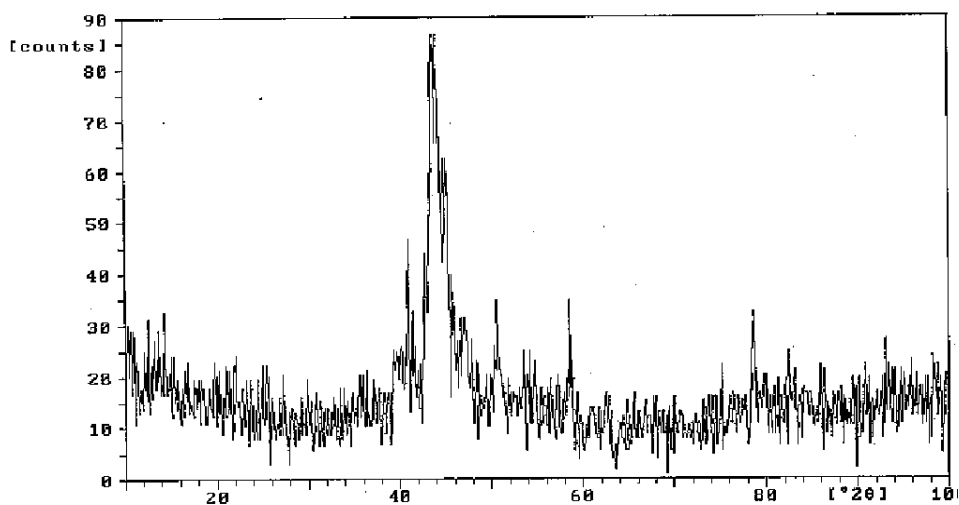


Figure 7. X-ray diffraction scan of the iron carbide catalyst following use for the conversion of 2-octanol at 275°C, 1 atm and LHSV = 3.2 h⁻¹.

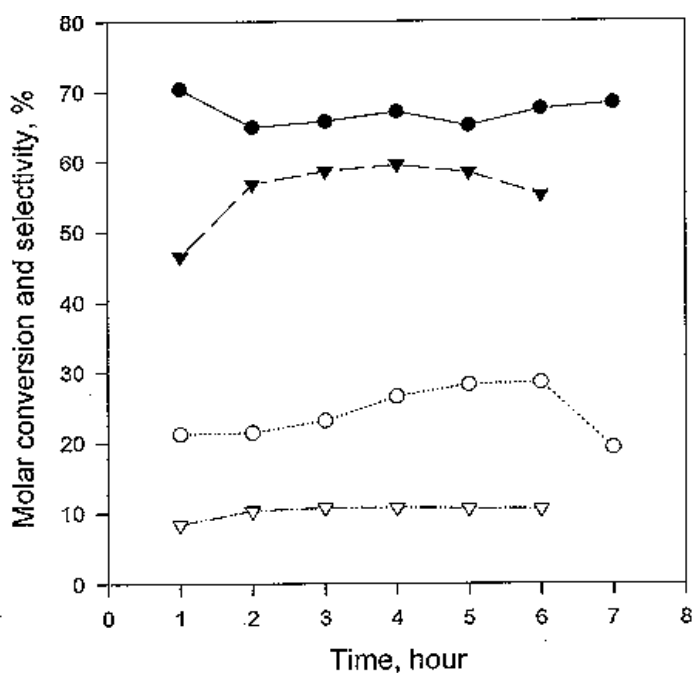


Figure 8. The conversion (▽; 275°C, 1 atm, LHSV = 3.3 h⁻¹) of 1-octanol with Fe₂O₃ and iron carbide (○; 275°C, 1 atm, LHSV = 3.3 h⁻¹) and the dehydrogenation selectivity to 1-octanal for Fe₂O₃ (▽) and iron carbide (●). [The low selectivity is due to formation of 8-pentadecanal from 1-octanal by secondary reactions].